

Chapter 7: An Imidazole-Based, Photolabile Structure-Directing Agent for the Synthesis of Aluminophosphate Zeolites

Abstract

The synthesis, photocleavage, and structure-directing ability of the photolabile molecule 1-(2-nitrobenzyl)-1H-imidazole (P-SDA 2) is presented and discussed. The organic molecule is synthesized via photochemical protection of the imidazole functionality by the 2-nitrobenzyl photochemical protecting group, and results in P-SDA 2 in approximately 30% overall yield. Photolytic cleavage of the molecule proceeds via long-wave UV radiation with an Hg arc lamp to generate the unstable 2-nitrosobenzyl derivative of the 2-nitrobenzyl photochemical protecting group and imidazole. The structure-directing ability of P-SDA 2 was evaluated via synthetic attempts to produce aluminophosphate zeolites, using procedures based on the syntheses of $\text{AlPO}_4\text{-5}$ (structure code AFI), VPI-5 (structure code VFI), and MAPO-34 (structure code CHA). In this case, a control molecule, 1-benzyl-1H-imidazole, a non-photoactive molecule designated as SDA 2, was used to screen conditions for the synthesis of aluminophosphate zeolites, resulting in the production of $\text{AlPO}_4\text{-5}$ (structure code AFI) and $\text{AlPO}_4\text{-36}$ (structure code ATS). This control molecule was also used to demonstrate the synthesis of MAPO-36 (structure code ATS) under metal-substituted, aluminophosphate synthetic conditions. Attempts to synthesize aluminophosphate zeolites with P-SDA 2 using conditions that produced microporous crystalline material with SDA 2 yielded several unknown, and likely mixed, crystalline phases, although the primary results of these syntheses were dense phases and hydrated phases. The addition

of magnesium to the synthesis, using MAPO-34 procedures, also resulted in the synthesis of unidentified crystalline materials, with P-SDA 2 still intact inside the framework. Complete photocleavage of P-SDA 2 within the crystalline, aluminophosphate materials was also demonstrated.

1. Introduction

As the use of zeolite in non-traditional applications increases, the need for alternative methods to liberate the pore space of zeolites also increases.^{1,2,3,4,5,6} Typically, thermal combustion processes are used to remove occluded organic molecules, but these processes destroy the often expensive structure-directing agent (SDA) within the zeolite pore space, and are frequently incompatible with either the end-use requirements or further fabrication steps of zeolites in nontraditional applications, like chemical sensors or electronic devices. Towards this end, the use of photolabile structure-directing agents for zeolite syntheses has been proposed, wherein the structure-directing agent can be removed post-synthesis via UV radiation and partially recycled.

To demonstrate the feasibility of the proposed route, a test molecule, 8,8-dimethyl-2-(2-nitrophenyl)-1,4-dioxo-8-azoniaspiro[4.5]decane hydroxide (P-SDA 1), a photo- and acid-cleavable organic molecule of the 2-nitrobenzyl family of photolabile molecules, was investigated in Chapter 6. This molecule was used to demonstrate that photocleavage of a molecule of the 2-nitrobenzyl family was possible in a large pore zeolite, such as a dealuminated zeolite with the FAU structure. Attempts to use this molecule to crystallize zeolites materials with the BEA* and MFI structures, using a wide

variety of synthesis conditions, however, resulted in only one of these syntheses producing a crystalline phase (MFI), which was not reproducible. The inability to reproducibly crystallize a zeolite might have been caused by the large structure of the P-SDA 1 molecule.

To address the problem of crystallization, a smaller member of the 2-nitrobenzyl family of photoactive compounds is proposed as a potential structure-directing agent: 1-(2-nitrobenzyl)-1H-imidazole (Figure 7.1a), known as P-SDA 2. Imidazole-based structure-directing agents have been used to synthesize a variety of zeolite phases, including zeolites with the ITW, MTT, TON, and MTW topologies, and other novel zeotype structures.^{7,8,9} Like all members of the 2-nitrobenzyl family, P-SDA 2 undergoes photolytic cleavage via an intramolecular hydrogen abstraction mechanism (Figure 7.2) when irradiated with light of wavelength 320 nm or longer. Additionally, many variations of the synthesis of P-SDA 2 exist in the literature; generally, these syntheses are steps on the path to more complex, polyfunctional molecules.^{10,11,12,13,14} Unlike P-SDA 1, P-SDA 2 is not acid-cleavable, making it suitable for acidic synthesis conditions, such as those used when crystallizing aluminophosphates zeolites, as well as basic synthesis conditions. Lastly, the non-photoactive equivalent of P-SDA 2, 1-benzyl-1H-imidazole (Aldrich, Figure 7.1b) is readily available and can be used to screen for the conditions that could potentially crystallize a zeolite material with P-SDA 2 (although previous work with P-SDA 1 has shown that the presence of a nitro substituent on the test molecule could affect its ability to act in a structure-directing role in comparison to the control molecule). For these reasons, the evaluation of the P-SDA 2 molecule in terms of

its structure-directing ability is of interest for the development of a photolabile route to zeolite synthesis.



Figure 7.1 (a) 1-(2-nitrobenzyl)-1H-imidazole (P-SDA 2) ; (b) 1-benzyl-1H-imidazole (SDA 2)

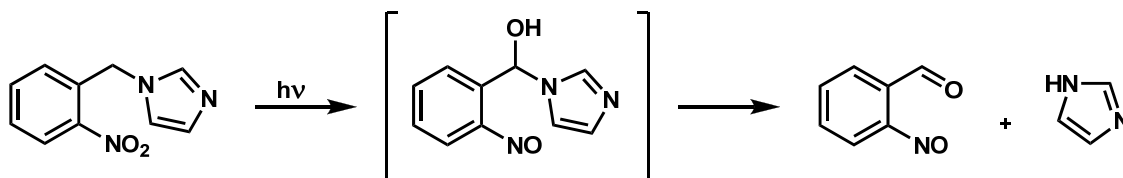


Figure 7.2 Photolysis of P-SDA 2 proceeds via an intramolecular hydrogen abstraction from the carbon-hydrogen bond ortho to the nitro group to yield carbonyl and nitroso groups in the ortho position

The stability of both P-SDA 2 and SDA 2 with respect to strong acids makes it possible to evaluate the molecules' potential structure-directing ability using the aluminophosphate class of zeolites, which crystallizes under acidic conditions. This family of crystalline, microporous materials is unusual in that crystallization of these

materials can occur in a matter of hours, rather than days, as with aluminosilicate zeolites.¹⁵ Aluminophosphate molecular sieves (AlPO₄'s) are generally crystallized from reactive gels of composition 1.0 Al₂O₃ / 1.0 (± 0.2) P₂O₅ / x SDA / y H₂O, where x is generally 1.0 – 3.0, and y is 20 – 100. The primary alumina source for these gels is pseudo-boehmite, a reactive, dense-phase, hydrated alumina powder; while the phosphorous source is o-phosphoric acid. Framework substitution of phosphorous for silicon, or metals such as magnesium, manganese, and iron for aluminum can also occur if the correct precursor gel and reaction conditions are used. Like aluminosilicate zeolites, the AlPO₄ materials crystallize at temperatures between 125 °C and 200 °C, but there are also notable differences. First, AlPO₄ materials have a neutral framework, due to the Al³⁺ and P⁵⁺ ions, consisting of alternating aluminum and phosphorous oxides, and therefore do not require charge-balancing cations. Instead, only water or organic molecules are present within the pore space. Second, AlPO₄ materials require the presence of an organic additive in the precursor gel in order to promote crystallization of stable, microporous materials. Third, the organic additive is generally less specific in its structure-directing role than for aluminosilicate zeolites in that a single aluminophosphate structure can be crystallized using an assortment of different structure-directing agents of various sizes, shapes, and solubility, while a single structure-directing agent can promote crystallization of a variety of aluminophosphate zeolite phases. For example, the aluminophosphate zeolite with the AlPO₄-5 structure can be synthesized with over 20 different nitrogen-containing organic additives.¹⁵ These additives can be primary, secondary, or tertiary amines, or the typical quaternary ammonium cations used for aluminosilicate zeolite synthesis. Fourth, dense aluminophosphate phases tend to form at

low crystallization temperatures in addition to high crystallization temperatures over long periods of time. These differences present three primary benefits for using the aluminophosphate zeolite system to evaluate the structure-directing ability of SDA 2 and P-SDA 2: (1) the fast crystallization time, (2) the ease of crystallization with a wide variety of structure-directing agents' sizes, shapes, etc., and (3) the standard precursor gel recipe, which reduces the variable space to be examined to variations of only two reagents (the structure-directing agent and water), in addition to crystallization time and temperature. In this chapter, the ability of SDA 2 and P-SDA 2 to synthesize aluminophosphate materials is examined and discussed. Additionally, a short study of the effects of gel composition and reaction temperature on the ability of SDA 2 to promote the crystallization of $\text{AlPO}_4\text{-36}$, the aluminophosphate zeolite with the ATS structure, is presented. Lastly, the ability of P-SDA 2 to undergo photolytic cleavage within crystalline aluminophosphate materials is demonstrated using procedures determined in Chapter 6.

2. Results and Discussion

2.1 P-SDA 2 Synthesis

The synthesis of P-SDA 2 was carried out according to literature procedures, generating the molecule in approximately 30% overall yield; general literature procedures reported yields of 17 – 30%.¹⁶ P-SDA 2 has several characteristic features in its infrared (IR) spectrum (Figure 7.3) and its ^{13}C cross-polarization, magic angle spinning, nuclear magnetic resonance (CPMAS NMR) spectrum (Figure 7.4). For instance, in the IR spectrum, the absorbances at 1530 and 1375 cm^{-1} are characteristic of the nitro group, and

in the ^{13}C spectrum, the peaks at 50 ppm and 145 ppm represent, respectively, the carbon attached to both the phenyl ring and the imidazole, and the carbon with the nitro substituent. These characteristic peaks may be used to verify that the molecule is still intact after crystallization. The thermogravimetric analysis (TGA) data indicate that there are two decomposition events, one beginning at 200 °C and the other beginning at 550 °C (Figure 7.5).

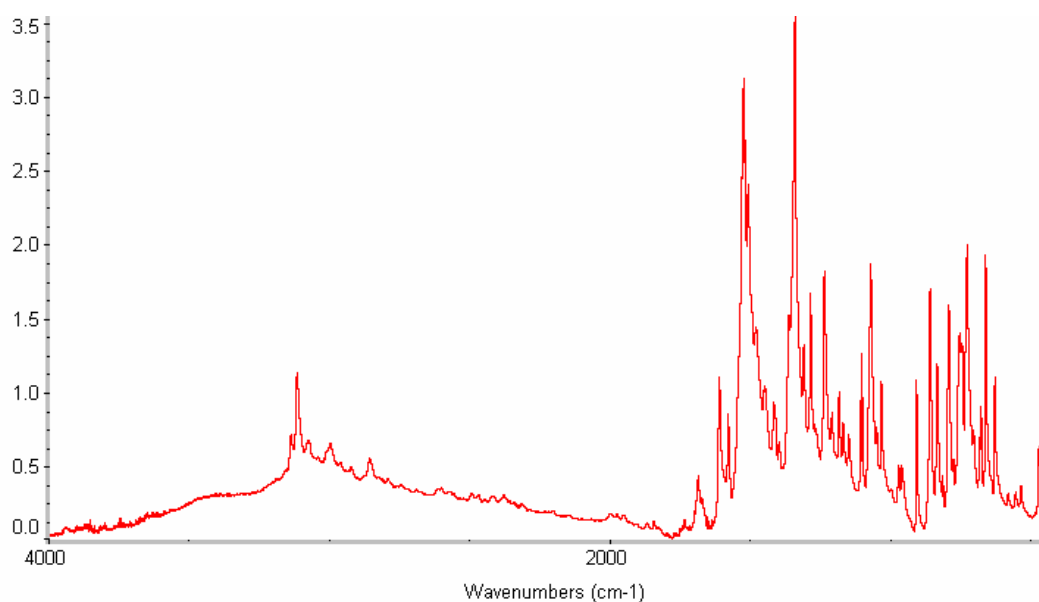


Figure 7.3 IR absorbance spectrum of P-SDA 2

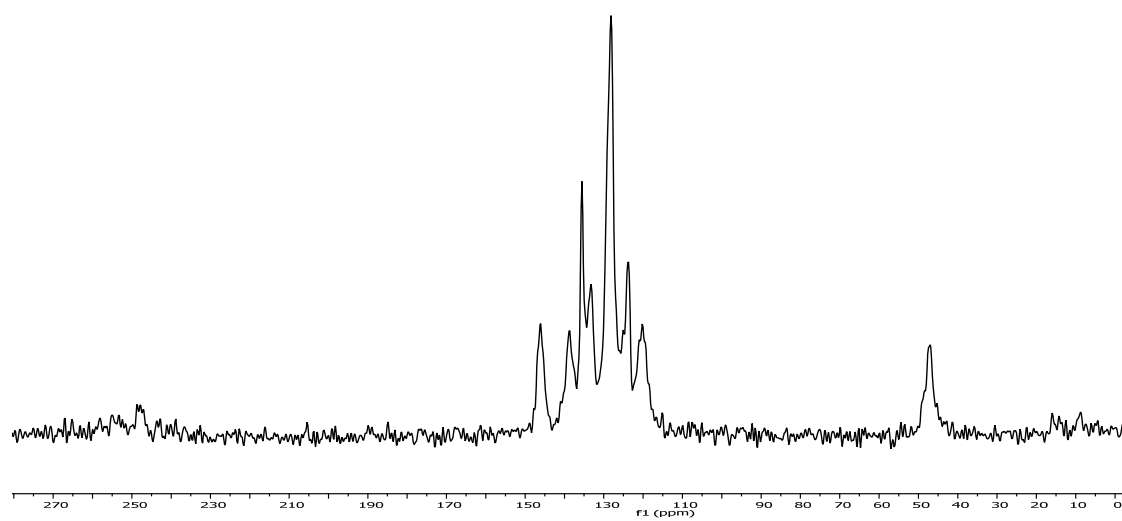


Figure 7.4 ^{13}C CP MAS NMR spectrum of P-SDA 2 at a spin rate of 6,000

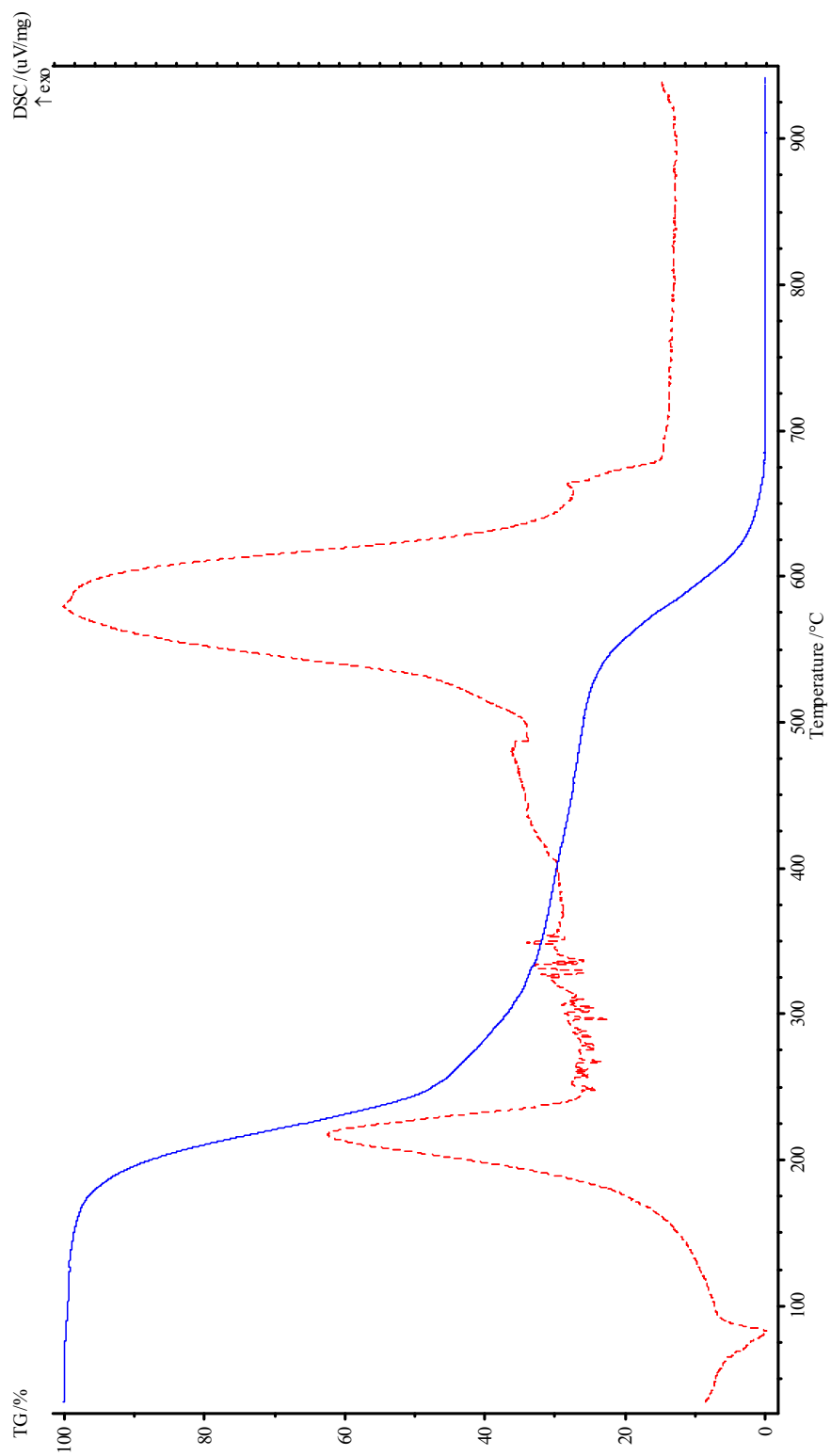


Figure 7.5 TGA data for P-SDA 2

2.2 Aluminophosphate Zeolite Synthesis Using SDA 2

The AlPO_4 control syntheses were designed to evaluate temperature, amount of structure-directing agent, and gel dilution, using molar gel compositions of $1 \text{ Al}_2\text{O}_3 / x \text{ SDA} / 1 \text{ P}_2\text{O}_5 / y \text{ H}_2\text{O}$ ($x = 1 - 3$, $y = 40, 60, 80$) and temperatures of 140, 150, and 200 °C. These procedures were based on the syntheses of AlPO_4 -5 (structure code AFI) and VPI-5 (structure code VFI). The results of the AlPO_4 syntheses attempted with SDA 2 are given in Table 7.1. The XRD patterns of the two phases obtained, AFI and ATS, are shown in Figure 7.6 (their corresponding structures are shown in Figure 7.7); in the XRD patterns both are mixed with other phases (a dense phase known as tridymite in the case of AFI, and an unknown phase for ATS). Interestingly, these phases formed only at 150 °C, and higher or lower temperatures yielded amorphous or dense phases.

To help guide the syntheses to a more conclusive crystalline phase, rather than a mixed phase, magnesium sulfate was introduced into the reactive aluminophosphate gel. The substitution of metals, such as magnesium, for the Al^{3+} atoms in the framework yields a more negatively charged framework, and can induce a “harder” positive charge on the amine functionality in the structure-directing agent.¹⁷ Several syntheses were run with a final molar gel composition of $0.8 \text{ Al}_2\text{O}_3 / 1 \text{ P}_2\text{O}_5 / x \text{ SDA} / y \text{ H}_2\text{O} / z \text{ MgO}$ where $x = 1 - 2$, $y = 10 - 100$, and $z = 0.2 - 0.4$, with the structure-directing agent being SDA 2. Table 7.2 shows the results of the various metal-substituted, aluminophosphate runs with SDA 2, and Figure 7.8 shows the XRD pattern that corresponds to the phases described in Table 7.2.

Table 7.1 Results of AlPO_4 syntheses attempted with SDA 2 (A = amorphous, DP = dense phase, #1 = ATS / unknown phase, #2 = AFI / tridymite)

Gel Composition	140 °C	150 °C	200 °C
1.0 Al_2O_3 / 1.0 P_2O_5 / 1.0 SDA / 40.0 H_2O	A	1	DP
1.0 Al_2O_3 / 1.0 P_2O_5 / 1.0 SDA / 60.0 H_2O	A	2	DP
1.0 Al_2O_3 / 1.0 P_2O_5 / 1.0 SDA / 80.0 H_2O	A	2	DP
1.0 Al_2O_3 / 1.0 P_2O_5 / 1.5 SDA / 40.0 H_2O	A	2	DP
1.0 Al_2O_3 / 1.0 P_2O_5 / 1.5 SDA / 60.0 H_2O	A	2	DP
1.0 Al_2O_3 / 1.0 P_2O_5 / 1.5 SDA / 80.0 H_2O	A	2	DP
1.0 Al_2O_3 / 1.0 P_2O_5 / 2.0 SDA / 40.0 H_2O	A	2	A
1.0 Al_2O_3 / 1.0 P_2O_5 / 2.0 SDA / 60.0 H_2O	A	2	A
1.0 Al_2O_3 / 1.0 P_2O_5 / 2.0 SDA / 80.0 H_2O	A	2	A
1.0 Al_2O_3 / 1.0 P_2O_5 / 2.5 SDA / 40.0 H_2O	A	A	A
1.0 Al_2O_3 / 1.0 P_2O_5 / 2.5 SDA / 60.0 H_2O	A	A	A
1.0 Al_2O_3 / 1.0 P_2O_5 / 2.5 SDA / 80.0 H_2O	A	2	A
1.0 Al_2O_3 / 1.0 P_2O_5 / 3.0 SDA / 40.0 H_2O	A	2	DP
1.0 Al_2O_3 / 1.0 P_2O_5 / 3.0 SDA / 60.0 H_2O	A	2	A
1.0 Al_2O_3 / 1.0 P_2O_5 / 3.0 SDA / 80.0 H_2O	A	2	A

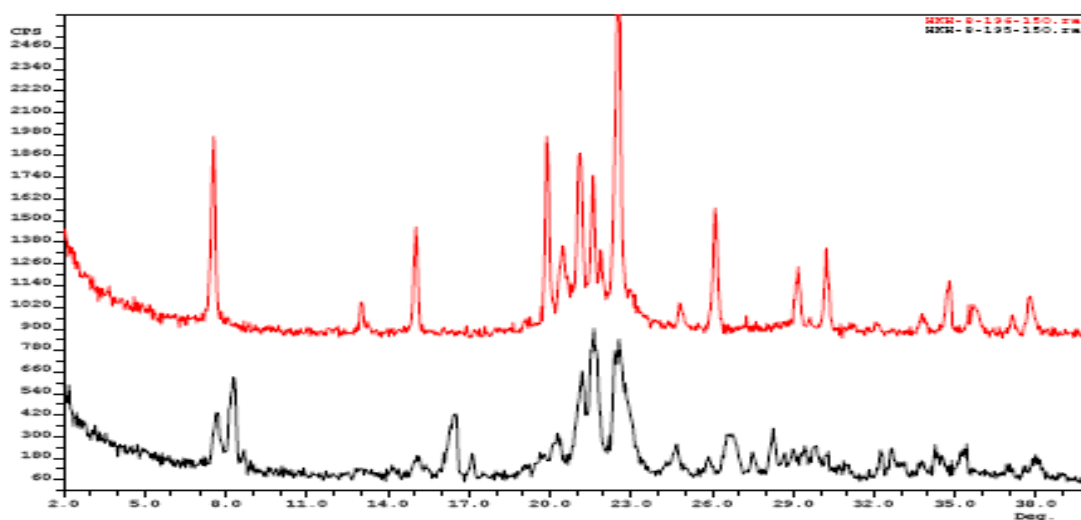


Figure 7.6 XRD patterns of aluminophosphate zeolites made with SDA 2: (bottom) ATS / unknown phase; (top) AFI / tridymite dense phase

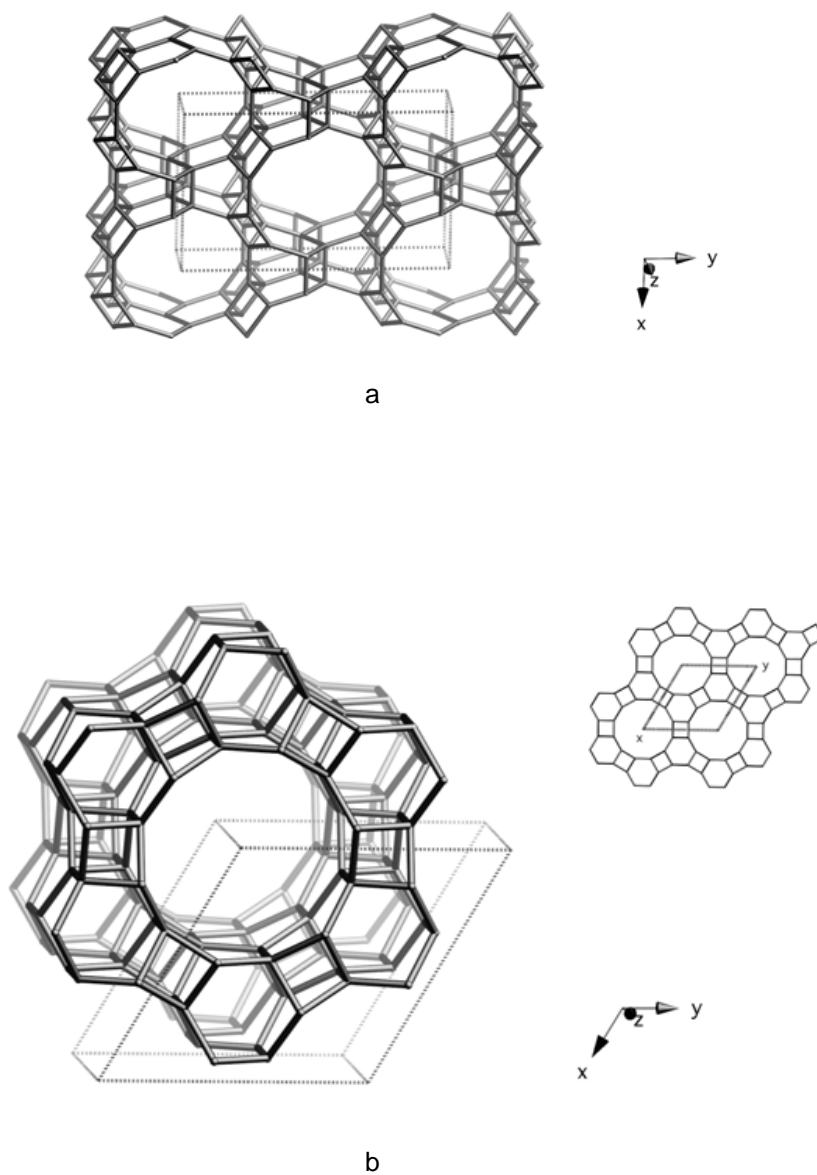


Figure 7.7 Framework schematic of the aluminophosphate zeolites phases: (a) ATS, viewed along the [001] axis; (b) AFI, viewed along the [001] axis with projection down the [001] axis on the upper right¹⁸

Table 7.2 Results of magnesium-substituted aluminophosphate runs using SDA 2 at 150, 175, and 200 °C (A = Amorphous)

Gel Composition	150 °C	175 °C	200 °C
0.8 Al ₂ O ₃ / 1.0 P ₂ O ₅ / 1.0 SDA / 10.0 H ₂ O / 0.2 MgO	ATS	ATS	A
0.8 Al ₂ O ₃ / 1.0 P ₂ O ₅ / 1.0 SDA / 10.0 H ₂ O / 0.4 MgO	ATS	ATS	ATS
0.8 Al ₂ O ₃ / 1.0 P ₂ O ₅ / 1.0 SDA / 47.0 H ₂ O / 0.2 MgO	ATS	ATS	ATS
0.8 Al ₂ O ₃ / 1.0 P ₂ O ₅ / 1.0 SDA / 47.0 H ₂ O / 0.4 MgO	ATS	ATS	A
0.8 Al ₂ O ₃ / 1.0 P ₂ O ₅ / 1.0 SDA / 100.0 H ₂ O / 0.2 MgO	ATS	ATS	ATS
0.8 Al ₂ O ₃ / 1.0 P ₂ O ₅ / 1.0 SDA / 100.0 H ₂ O / 0.4 MgO	ATS	ATS	ATS
0.8 Al ₂ O ₃ / 1.0 P ₂ O ₅ / 1.5 SDA / 10.0 H ₂ O / 0.2 MgO	ATS	ATS	ATS
0.8 Al ₂ O ₃ / 1.0 P ₂ O ₅ / 1.5 SDA / 10.0 H ₂ O / 0.4 MgO	ATS	ATS	ATS / AFI
0.8 Al ₂ O ₃ / 1.0 P ₂ O ₅ / 1.5 SDA / 47.0 H ₂ O / 0.2 MgO	ATS	ATS	ATS
0.8 Al ₂ O ₃ / 1.0 P ₂ O ₅ / 1.5 SDA / 47.0 H ₂ O / 0.4 MgO	ATS	ATS	A
0.8 Al ₂ O ₃ / 1.0 P ₂ O ₅ / 1.5 SDA / 100.0 H ₂ O / 0.2 MgO	ATS	ATS	A
0.8 Al ₂ O ₃ / 1.0 P ₂ O ₅ / 1.5 SDA / 100.0 H ₂ O / 0.4 MgO	ATS	ATS	ATS
0.8 Al ₂ O ₃ / 1.0 P ₂ O ₅ / 2.0 SDA / 10.0 H ₂ O / 0.2 MgO	ATS	A	A
0.8 Al ₂ O ₃ / 1.0 P ₂ O ₅ / 2.0 SDA / 10.0 H ₂ O / 0.4 MgO	ATS	ATS	AFI
0.8 Al ₂ O ₃ / 1.0 P ₂ O ₅ / 2.0 SDA / 47.0 H ₂ O / 0.2 MgO	A	ATS	ATS
0.8 Al ₂ O ₃ / 1.0 P ₂ O ₅ / 2.0 SDA / 47.0 H ₂ O / 0.4 MgO	ATS	ATS	ATS
0.8 Al ₂ O ₃ / 1.0 P ₂ O ₅ / 2.0 SDA / 100.0 H ₂ O / 0.2 MgO	ATS	ATS	A
0.8 Al ₂ O ₃ / 1.0 P ₂ O ₅ / 2.0 SDA / 100.0 H ₂ O / 0.4 MgO	ATS	ATS	ATS

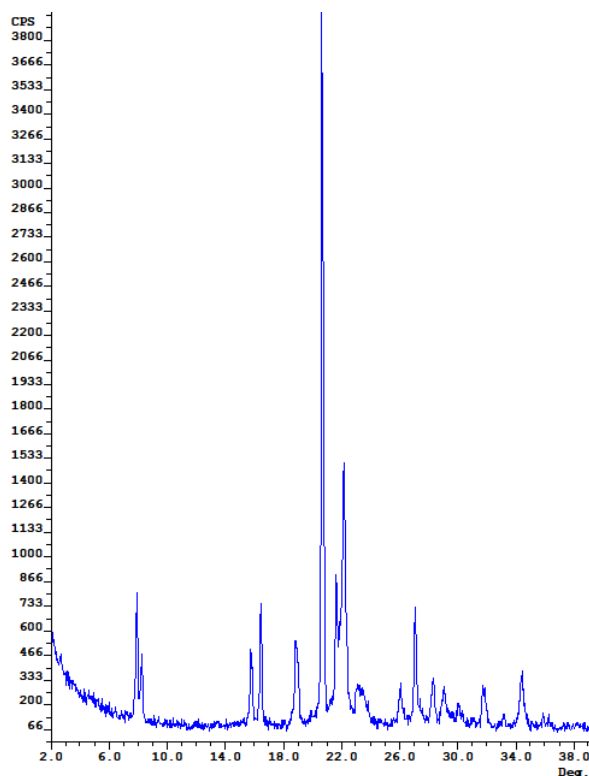


Figure 7.8 XRD pattern of the ATS phase from the compositions in Table 7.2

Some general trends can be seen in the results of the syntheses. (a) Aluminophosphate materials with the zeolite structure ATS are the preferred crystallization product of these syntheses with SDA 2. (b) Gels that were crystallized at 200 °C yielded approximately 1/3 of the crystalline material as the 175 °C runs, and were more frequently amorphous. (c) A shift between the production of aluminophosphate materials with the zeolite structures of ATS and AFI can be seen at 200 °C for higher amounts of magnesium in the synthesis. (d) At 150 °C, higher magnesium content in the zeolite gel leads higher crystallinity in the resulting materials, as the diffraction patterns of those materials are more intense with sharper peaks, but otherwise does not appear to change the structure that is crystallized. Given this data, it is apparent that attempts to synthesize aluminophosphate zeolites with P-SDA 1 could lead to the production of materials with

the ATS zeolite structure at 150 °C; additionally, using the lower temperature conditions would minimize the possibility of thermal decomposition of the P-SDA 2 molecule.

2.3 Aluminophosphate Zeolite Synthesis Using P-SDA 2

After identifying the synthesis conditions likely to produce aluminophosphate zeolite materials with SDA 2, the reactive precursor gels were modified to utilize P-SDA 2 as the structure-directing agent. Four different crystalline materials were produced from the syntheses (Table 7.3, Figure 7.9). These phases were designated as phases 3, 4, 5, 6, and 7. Phase 3 was a hydrated phase that collapses on dehydration to form a dense material. The other three phases were not readily identifiable as known crystalline materials, and were likely the result of mixed phases; phase 5, however, could potentially be a combination of ATS and another unknown phase. Interestingly, on calcination, phase 5 transformed into an aluminophosphate material with the zeolite structure ATV, in addition to some slight dense phase impurities. From these data, the following conclusions were reached regarding the production of the hydrate phase (phase 3): (a) gels containing higher P_2O_5 / Al_2O_3 ratios were more likely to yield a hydrated phase or dense phases, (b) at low P_2O_5 / Al_2O_3 ratios in the gel, a lower P-SDA 2 content will more likely result in a hydrated phase than a non-hydrate, crystalline phase, and (c) generally, gels that are more dilute are more likely to produce hydrated phases, while more concentrated phases will produce a non-hydrate, crystalline phase.

Table 7.3 Results of attempted aluminophosphate zeolite syntheses with P-SDA 2 as the structure-directing agent (3 = unknown hydrated phase, 4 = unknown phase, 5 = unknown phase, 6 = ATS / unknown phase, 7 = ATV / dense phase, DP = dense phase)

Gel Composition	150 °C	Calcined
1.0 Al ₂ O ₃ / 1.0 P ₂ O ₅ / 1.0 SDA / 40.0 H ₂ O	3	DP
1.0 Al ₂ O ₃ / 1.0 P ₂ O ₅ / 1.0 SDA / 50.0 H ₂ O	DP	DP
1.0 Al ₂ O ₃ / 1.0 P ₂ O ₅ / 1.0 SDA / 60.0 H ₂ O	3	DP
1.0 Al ₂ O ₃ / 1.0 P ₂ O ₅ / 1.0 SDA / 80.0 H ₂ O	3	DP
1.0 Al ₂ O ₃ / 1.0 P ₂ O ₅ / 1.5 SDA / 40.0 H ₂ O	3	DP
1.0 Al ₂ O ₃ / 1.0 P ₂ O ₅ / 1.5 SDA / 60.0 H ₂ O	3	DP
1.0 Al ₂ O ₃ / 1.0 P ₂ O ₅ / 1.5 SDA / 80.0 H ₂ O	3	DP
1.0 Al ₂ O ₃ / 1.0 P ₂ O ₅ / 2.0 SDA / 40.0 H ₂ O	4	4
1.0 Al ₂ O ₃ / 1.0 P ₂ O ₅ / 2.0 SDA / 40.0 H ₂ O	5	7
1.0 Al ₂ O ₃ / 1.0 P ₂ O ₅ / 2.0 SDA / 60.0 H ₂ O	4	4
1.0 Al ₂ O ₃ / 1.0 P ₂ O ₅ / 2.0 SDA / 60.0 H ₂ O	5	7
1.0 Al ₂ O ₃ / 1.0 P ₂ O ₅ / 2.0 SDA / 80.0 H ₂ O	4	4
1.0 Al ₂ O ₃ / 1.0 P ₂ O ₅ / 2.0 SDA / 80.0 H ₂ O	5	7
1.0 Al ₂ O ₃ / 1.0 P ₂ O ₅ / 2.5 SDA / 40.0 H ₂ O	4	4
1.0 Al ₂ O ₃ / 1.0 P ₂ O ₅ / 2.5 SDA / 60.0 H ₂ O	4	4
1.0 Al ₂ O ₃ / 1.0 P ₂ O ₅ / 2.5 SDA / 80.0 H ₂ O	5	7
1.0 Al ₂ O ₃ / 1.0 P ₂ O ₅ / 3.0 SDA / 40.0 H ₂ O	4	4
1.0 Al ₂ O ₃ / 1.0 P ₂ O ₅ / 3.0 SDA / 60.0 H ₂ O	4	4
1.0 Al ₂ O ₃ / 1.0 P ₂ O ₅ / 3.0 SDA / 80.0 H ₂ O	4	4
1.0 Al ₂ O ₃ / 1.5 P ₂ O ₅ / 0.5 SDA / 40.0 H ₂ O	3	DP
1.0 Al ₂ O ₃ / 1.5 P ₂ O ₅ / 0.75 SDA / 10.0 H ₂ O	5	7
1.0 Al ₂ O ₃ / 1.5 P ₂ O ₅ / 0.75 SDA / 40.0 H ₂ O	6	-
1.0 Al ₂ O ₃ / 1.5 P ₂ O ₅ / 0.75 SDA / 50.0 H ₂ O	3	DP

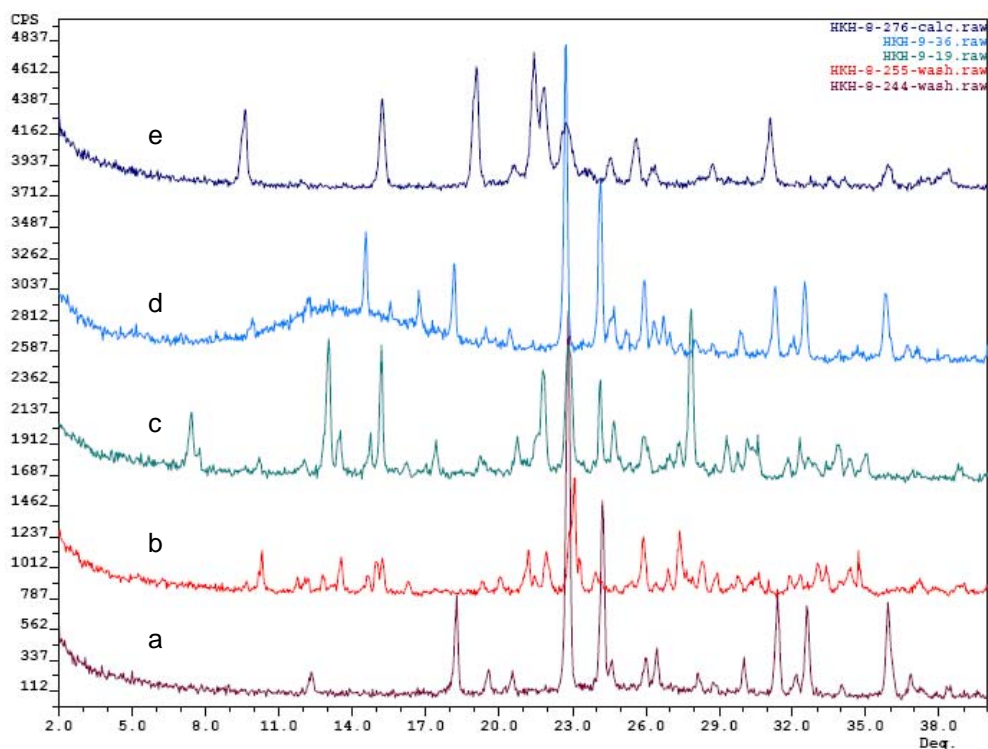


Figure 7.9 XRD patterns of as-made aluminophosphate materials produced using P-SDA 2 as the structure-directing agent: (a) phase 3; (b) phase 4; (c) phase 5; (d) phase 6; and calcined phase 5: (e) ATV / dense phase

Of the conditions in Table 7.3, those that produced phases 4 and 5 appeared most likely to promote the reproducible crystallization of known aluminophosphate zeolite phases rather than dense phases, so the resulting crystalline material was further investigated. According to the ^{13}C CP MAS NMR spectrum of the phase 5 material (Figure 7.10), P-SDA 2 is still intact. TGA data of the phase (Figure 7.11) show similar decomposition events as the P-SDA itself, with a reasonable organic content for an aluminophosphate material.

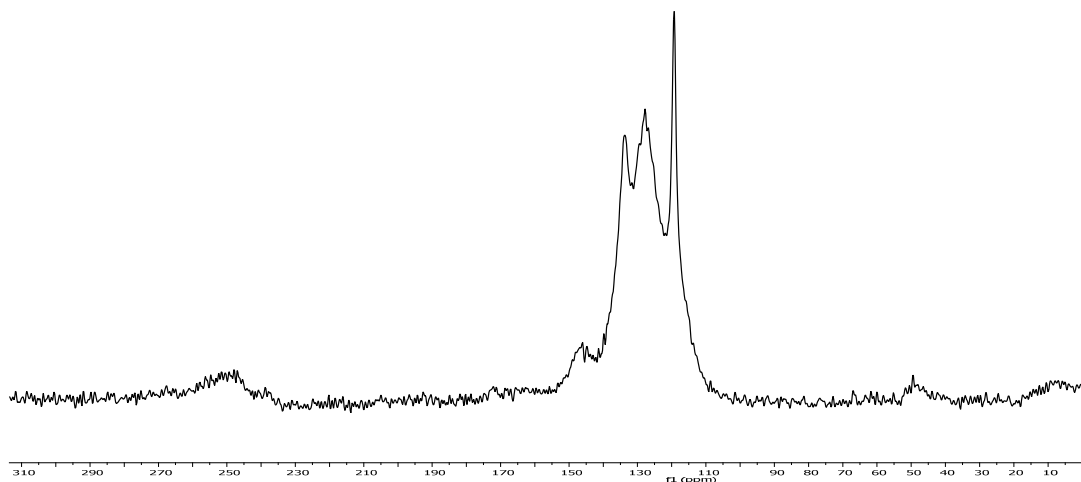


Figure 7.10 ^{13}C CPMAS NMR spectrum of the as-made, crystalline, aluminophosphate phase 5 produced using P-SDA 2 as the structure-directing agent

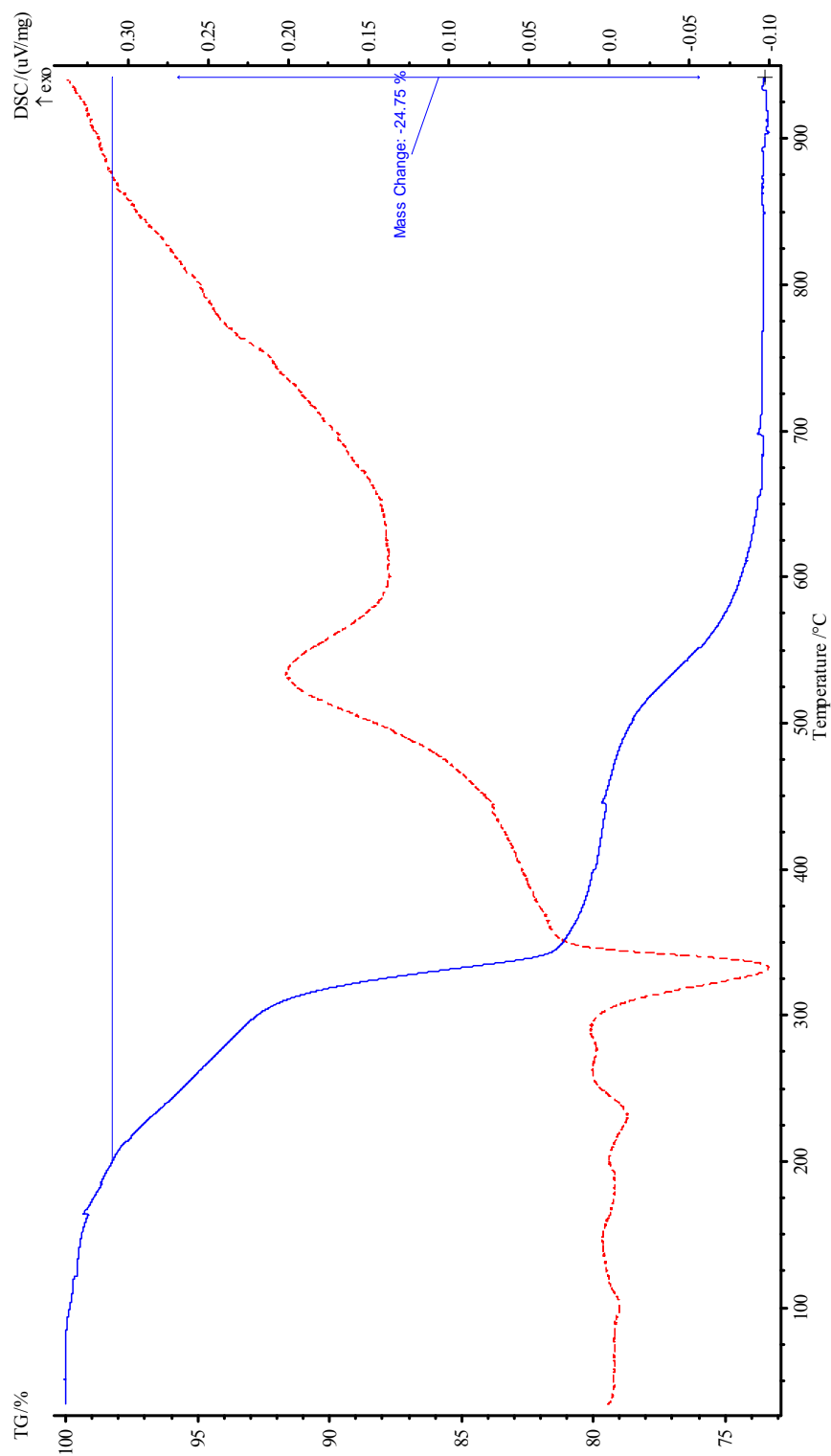


Figure 7.11 TGA data of the as-made, aluminophosphate phase 5, produced using P-SDA 2 as the structure-directing agent

The results shown above demonstrate that P-SDA 2 is indeed capable of acting in a structure-directing role for the synthesis of crystalline, aluminophosphate materials and withstanding the conditions of an aluminophosphate zeolite synthesis. However, the results also demonstrate its lack of specificity towards any one phase; interestingly, the same reaction conditions produced both phase 4 and phase 5. In order to guide the synthesis of aluminophosphate materials in such a way that a more definite crystalline material is formed using P-SDA 2 as the structure-directing agent, the synthetic conditions were modified to include metal substitution. As with SDA 2, metal-substituted aluminophosphates were synthesized with a final molar gel composition of $0.8 \text{ Al}_2\text{O}_3 / x \text{ SDA} / 1 \text{ P}_2\text{O}_5 / y \text{ H}_2\text{O} / z \text{ MgO}$ where $x = 1 - 2$, $y = 47 - 100$, and $z = 0.2 - 0.4$ using P-SDA 2 as the structure-directing agent, at temperatures of 150 and 175 °C. The results of these synthetic attempts are shown in Table 7.4

These results demonstrate that a crystallization temperature of 150 °C results in the production of crystalline material using P-SDA 2 as the structure-directing agent, compared to higher temperatures. Additionally, the magnesium substitution does not appear to promote the crystallization of a specific phase or known material, and instead narrows the results to phases 4 and 5 (Figure 7.9). Lastly, the difference in water content greatly affects the results, as more dilute gels produced dense phases with greater regularity than concentrated gels. Therefore, aluminophosphate materials can be produced using relatively mild synthetic conditions and P-SDA 2 as the structure-directing agent; however, these aluminophosphates are not known zeolite phases.

Table 7.4 Results of attempted metal-substituted, aluminophosphate zeolite syntheses with P-SDA 2 as the structure-directing agent

Gel Composition	150 °C	175 °C
0.8 Al ₂ O ₃ / 1.0 P ₂ O ₅ / 1.0 SDA / 47.0 H ₂ O / 0.2 MgO	5	A
0.8 Al ₂ O ₃ / 1.0 P ₂ O ₅ / 1.0 SDA / 100.0 H ₂ O / 0.2 MgO	DP	DP
0.8 Al ₂ O ₃ / 1.0 P ₂ O ₅ / 1.5 SDA / 47.0 H ₂ O / 0.2 MgO	5	4
0.8 Al ₂ O ₃ / 1.0 P ₂ O ₅ / 1.5 SDA / 100.0 H ₂ O / 0.2 MgO	DP	5
0.8 Al ₂ O ₃ / 1.0 P ₂ O ₅ / 2.0 SDA / 47.0 H ₂ O / 0.2 MgO	5	A
0.8 Al ₂ O ₃ / 1.0 P ₂ O ₅ / 2.0 SDA / 100.0 H ₂ O / 0.2 MgO	DP	DP
0.8 Al ₂ O ₃ / 1.0 P ₂ O ₅ / 1.0 SDA / 47.0 H ₂ O / 0.4 MgO	DP	DP
0.8 Al ₂ O ₃ / 1.0 P ₂ O ₅ / 1.0 SDA / 100.0 H ₂ O / 0.4 MgO	DP	DP
0.8 Al ₂ O ₃ / 1.0 P ₂ O ₅ / 1.5 SDA / 47.0 H ₂ O / 0.4 MgO	A	DP
0.8 Al ₂ O ₃ / 1.0 P ₂ O ₅ / 1.5 SDA / 100.0 H ₂ O / 0.4 MgO	4 / 5	4 / 5
0.8 Al ₂ O ₃ / 1.0 P ₂ O ₅ / 2.0 SDA / 47.0 H ₂ O / 0.4 MgO	A	4
0.8 Al ₂ O ₃ / 1.0 P ₂ O ₅ / 2.0 SDA / 100.0 H ₂ O / 0.4 MgO	DP	DP

2.4 Photocleavage of P-SDA 2 within Aluminophosphate Material

Samples of the aluminophosphate materials generated using P-SDA 2 were subjected to UV radiation in an attempt to photolytically cleave P-SDA 2 in the pores, using thin layer procedures developed previously. The ¹³C CP MAS NMR spectrum (Figure 7.12) showed that the P-SDA 2 material was completely cleaved, as evidenced by the disappearance of the peak at 50 ppm. Additionally, the spectrum contained only those peaks that would correspond to the imidazole fragment.

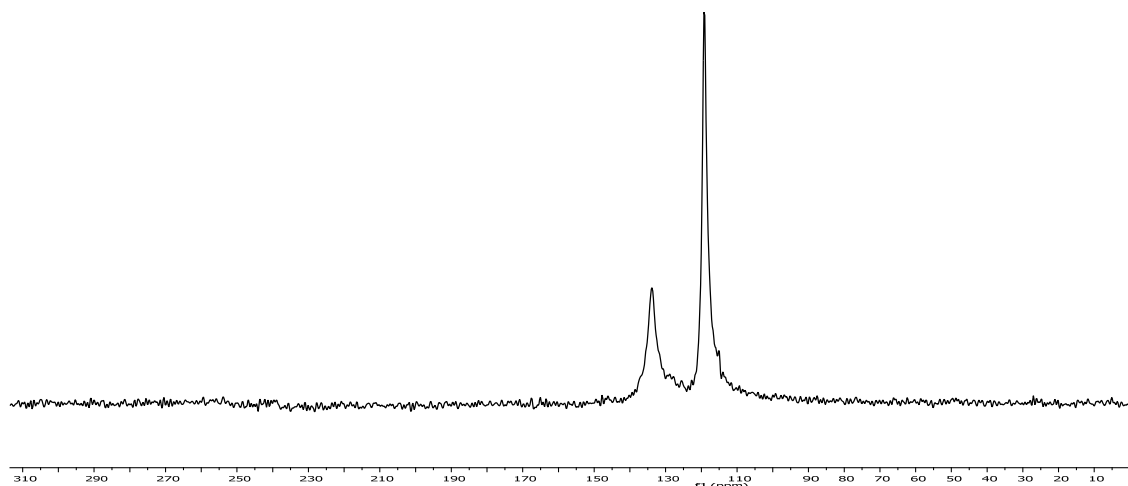


Figure 7.12 ^{13}C CPMAS NMR spectrum of as-made, aluminophosphate material produced using P-SDA 2 as the structure-directing agent, after UV irradiation

Initial attempts to extract the cleaved fragment were partially successful, as the color of the sample lightened from a deep red / brown to a light tan, however, further testing via NMR revealed that organic was still present in the irradiated sample. Further extraction processes, such as soxhlet extraction with polar solvents such as acetone, ethylacetate, and water, completely removed approximately 35% of the remaining imidazole fragment according to TGA data (Figure 7.13). XRD analysis of the cleaved and extracted material showed that the phase remained intact after these processing steps (Figure 7.14). The inability to completely remove the imidazole fragment suggests that, if the material is porous, the pore apertures of the structure may be too small to allow access to the imidazole fragment. Alternatively, the imidazole fragment could be protonated and bound to the framework via electrostatic interactions to charge-balance defects in the structure. Protonated imidazoles generally show broad features in the $3000\text{-}3500\text{ cm}^{-1}$ region of their IR spectra; these can be seen in the remaining imidazole fragments in the

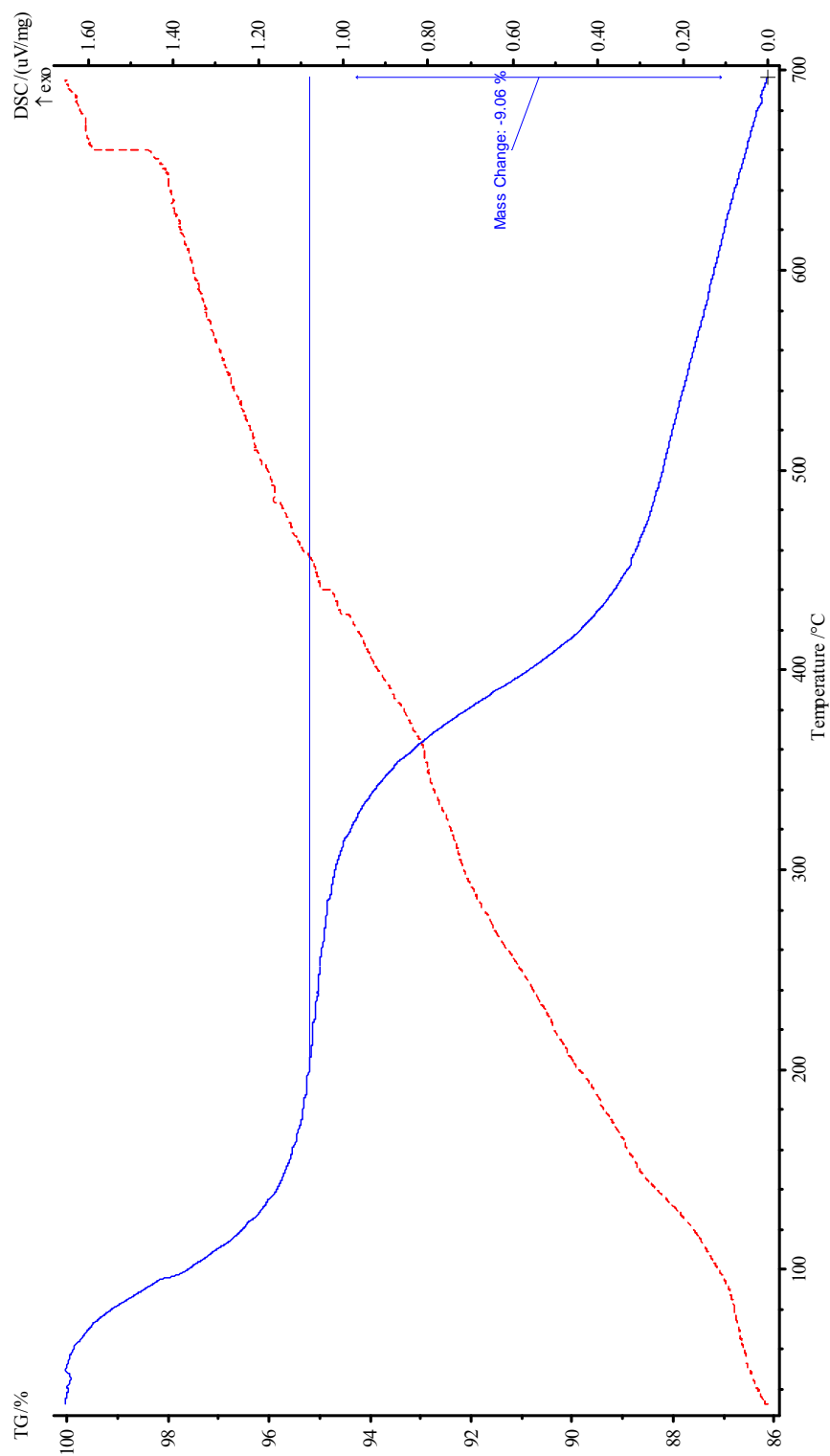


Figure 7.13 TGA data of the cleaved and extracted aluminophosphate material

extracted phase 5 material (Figure 7.15), suggesting that this is the case.

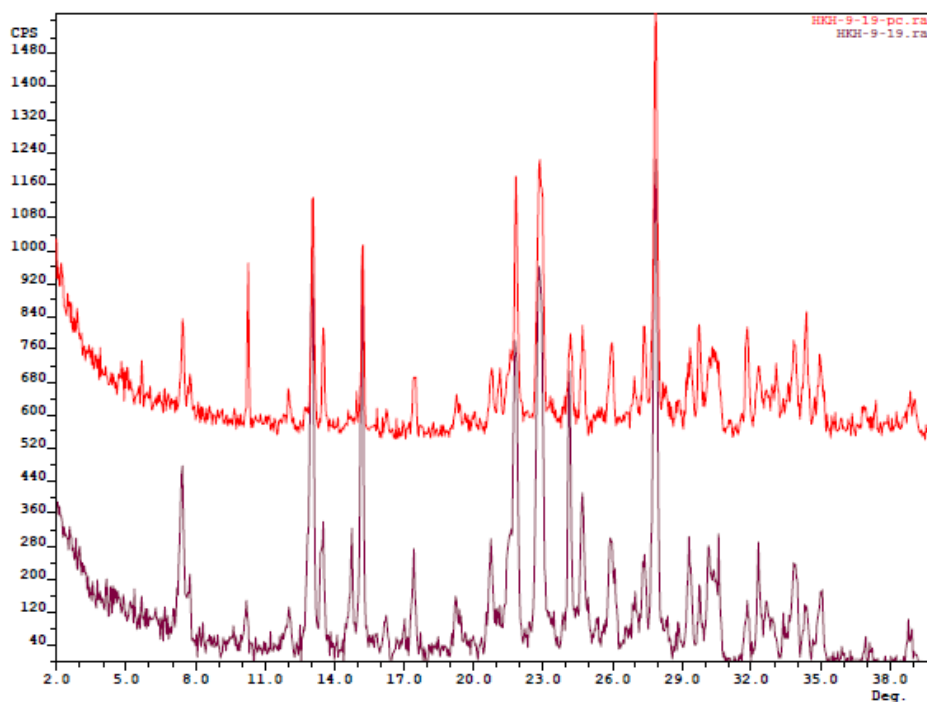


Figure 7.14 XRD patterns of: (bottom) the as-made phase 5 sample; (top) the photocleaved phase 5 sample

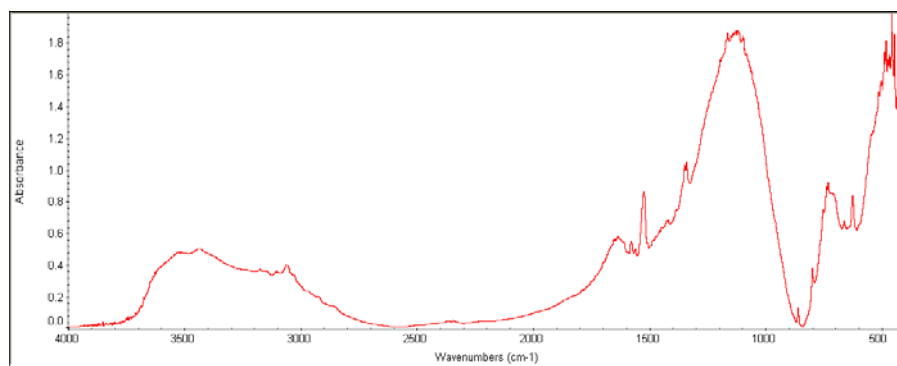


Figure 7.15 IR spectra of photocleaved and extracted phase 5 sample

Given that the as-made material undergoes a transformation to an ATV / dense phase material upon high temperature calcination, but remains in the as-made crystalline structure on photocleavage, we were interested in comparing the resulting materials. The phase transformation of an aluminophosphate material to ATV on high temperature calcination is not unusual, as this typically occurs during the calcination of $\text{AlPO}_4\text{-21}$ (structure code AWO). Scanning electron microscope micrographs of the photocleaved material (Figure 7.16a) and the ATV-like material that is formed on high-temperature calcination (Figure 7.16b) show that the crystals do not have an obvious crystal habit, with crystal sizes ranging from sub-micron to tens of microns. It is, of course, possible that the phase 5 material is a mixed phase, thus accounting for the range of crystal sizes and lack of definite crystal habit; in fact, many of the sub-micron to micron-sized crystals appear to be in a flat plate conformation. The calcined ATV / dense phase material looks very similar to the phase 5 material, in that there is no obvious crystal habit, although on the whole, the crystals for this phase are larger than that of the phase 5 material.

Nitrogen adsorption measurements of the ATV / dense phase sample showed that the sample has 0.034 cc pore / g sample, of which 0.009 cc / g is due to microporosity, which is very low for zeolite materials. Interestingly, literature reports of the porosity of ATV materials state that the apertures of the ATV structure (3.0 Å by 4.9 Å) are either too distorted or too small to readily adsorb N_2 , which explains the low porosity obtained.¹⁹

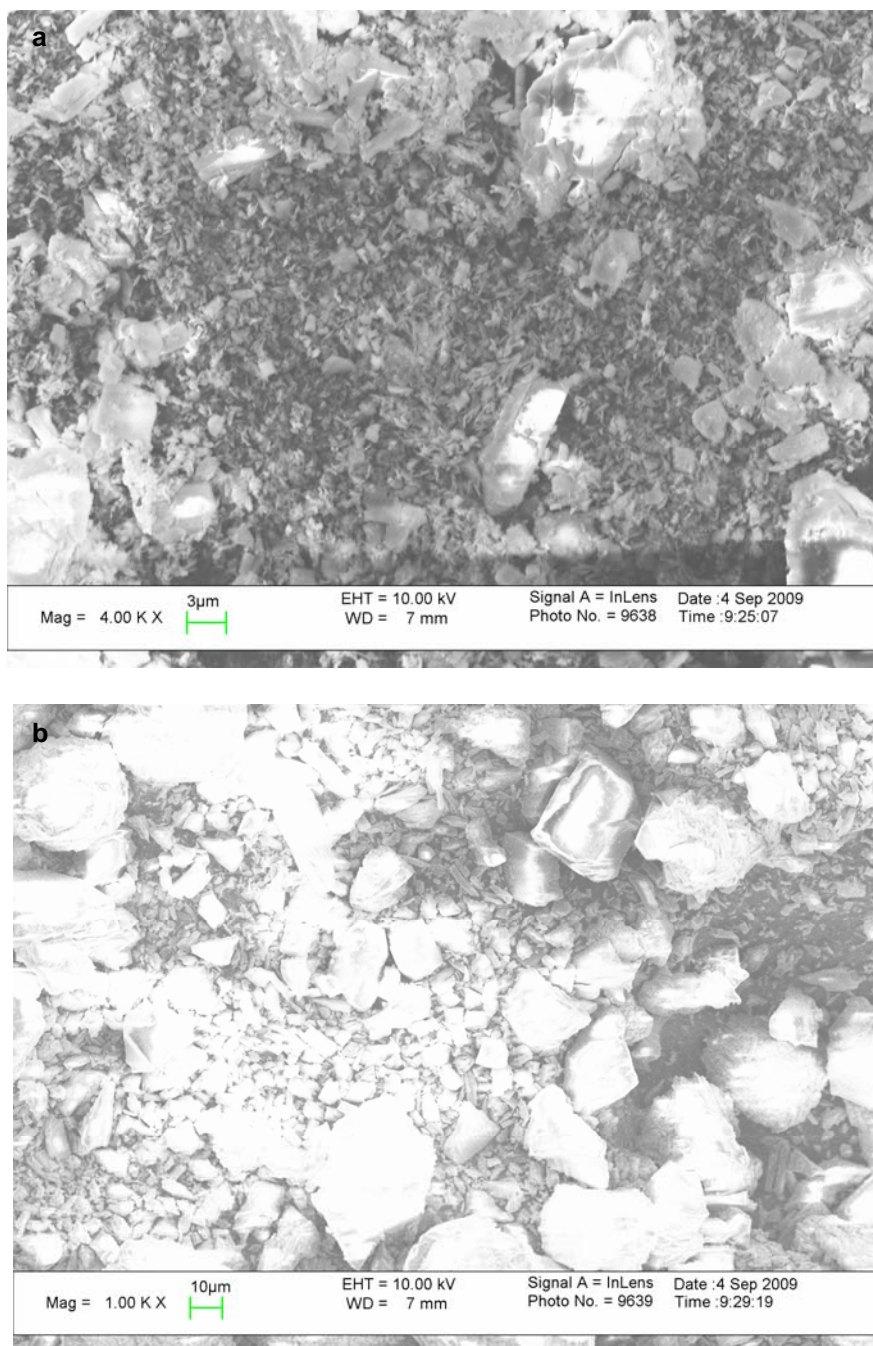


Figure 7.16 SEM micrographs of: (a) photocleaved phase 5 crystals and aggregates; (b) calcined ATV / dense phase material crystals and aggregates

3. Conclusions

The use of the photolabile molecule 1-(2-nitrobenzyl)-1H-imidazole (P-SDA 2) as a structure-directing agent in aluminophosphate and metal-substituted aluminophosphate zeolite syntheses resulted in the formation of crystalline aluminophosphate materials with unknown structures, potentially including the zeolite structure ATS. In general, the ability of this molecule to act in a structure-directing role for the production of aluminophosphate materials was confirmed; however, its ability to act as a structure-directing agent for aluminophosphate zeolites was not confirmed. Unlike many structure-directing agents, this molecule does not promote the crystallization of only one crystalline phase, rather, it can promote crystallization of a variety of materials. The addition of magnesium to the aluminophosphate reactive gels, however, narrowed the range of aluminophosphate phases produced to only two: phase 4 and phase 5. The latter of these could include material with the zeolite structure ATS. On calcination, the crystalline aluminophosphates with phase 5 produced materials with the zeolite structure ATV. The complete photocleavage of P-SDA 2 within the aluminophosphate materials was also demonstrated. Overall, the feasibility of a photolabile structure-directing agent route to the synthesis of crystalline aluminophosphates, rather than aluminophosphate zeolites, was demonstrated. This method could therefore provide a reasonable substitute for calcination for materials that require an organic additive to be crystallized, and can be formed with photolabile organic additives.

4. Experimental

4.1 Synthesis of P-SDA 2

P-SDA 2 was synthesized following literature procedures using standard S_N2 chemistry to protect the amino functionality of imidazole (Figure 7.14).¹²

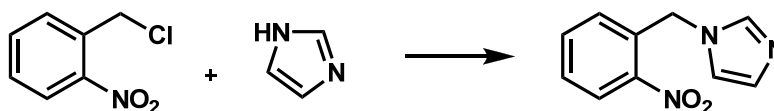


Figure 7.17 Synthesis of P-SDA 2 via photochemical protection of the amino functionality of the imidazole

13.44 g of 2-nitrobenzylchloride (Aldrich) and 7.05 g of imidazole (sodium derivative, Acros) were combined in a 500 mL round-bottom flask equipped with a stirbar and covered in aluminum foil. A condenser was placed in the flask, which was then placed under an Ar atmosphere in an oil bath. Approximately 250 mL of anhydrous 1,2-dimethoxyethane (EMD) was added via syringe techniques to the flask, and the solution was refluxed at 90 °C for up to 12 h. The solution was filtered to remove the NaCl evolved, as well as unreacted reagents, and the solids were washed thoroughly with chloroform to fully remove any product in the solids. The filtrate was then rotovapped to remove the solvent, and 30 mL distilled, deionized (DDI) H₂O was added to dissolve the solids. The crude product was extracted from the aqueous phase with four washings of 50 mL ethyl acetate each, using a separation funnel. The organic phase was collected and evaporated using a rotovap to give a viscous orange to deep red liquid. The crude

product was recrystallized from ether, or toluene / ether to produce red crystals in approximately 30% yield.

4.2 Synthesis of Aluminophosphate Zeolites with SDA 2 and P-SDA 2

Aluminophosphates were synthesized with a final molar gel composition of $1 \text{ Al}_2\text{O}_3 / x \text{ SDA} / 1 \text{ P}_2\text{O}_5 / y \text{ H}_2\text{O}$ where $x = 1, 1.5, 2, 2.5, \text{ and } 3$ and $y = 40, 60, \text{ and } 80$. The structure-directing agent for these syntheses was either 1H-benzylimidazole (Aldrich, SDA 2), or 1-(2-nitrobenzyl)-1H-imidazole (P-SDA 2). These gels were created by first dissolving o-phosphoric acid (85 wt%, Fisher) in DDI H_2O (~ 30 wt % of the total DDI H_2O added) in a Teflon jar and adding the stirred solution to a suspension of $\text{Al}_2\text{O}_3 \cdot 2\text{H}_2\text{O}$ (Catapal Alumina Vista) in DDI H_2O (~ 70 wt% of the total DDI H_2O added) that had been stirred for 10 m. After combining, the slurry was stirred at room temperature for 2 h. The SDA was then added to the slurry, and the gel was then stirred for at least 1.5 h. The homogeneous gel was then crystallized, until phase separation at 140, 150, 175, or 200 °C in a Teflon-lined Parr autoclave, usually 48 – 96 hours. After removing the autoclave from the oven, the product was slurried in 35 mL of DDI H_2O in a 50 mL centrifuge tube, and the solution was centrifuged and decanted. The resulting solids were slurried with 35 mL of acetone (Fisher), and centrifuged several times, until the supernatant was clear. The solids were then air-dried at 100 °C overnight.

4.3 Synthesis of Metal-Substituted Aluminophosphate Zeolites with SDA 2 and P-SDA

2

Metal-substituted aluminophosphates were synthesized with a final molar gel composition of $0.8 \text{ Al}_2\text{O}_3 / x \text{ SDA} / 1 \text{ P}_2\text{O}_5 / y \text{ H}_2\text{O} / z \text{ MgO}$ where $x = 1 - 2$, $y = 10 - 100$, and $z = 0.2 - 0.4$. The structure-directing agent for these syntheses was either 1H-benzylimidazole (Aldrich, SDA 2), or 1-(2-nitrobenzyl)-1H-imidazole (P-SDA 2). These gels were created by first dissolving o-phosphoric acid (85 wt%, Fisher) in DDI H₂O (~30 wt % of the total DDI H₂O added) in a Teflon jar and adding to the stirred solution $\text{Al}_2\text{O}_3 \cdot 2\text{H}_2\text{O}$ (Catapal Alumina Vista). After combining, the slurry was stirred at room temperature for 2 h. The SDA was then added to the slurry, and the gel was then stirred for another 2 h. The metal (anhydrous magnesium sulfate) was added, and the gel was stirred again for 2 h. The homogeneous gel was then crystallized, until phase separation at 150, 175, or 200 °C in a Teflon-lined Parr autoclave, usually 24 - 72 h. After removing the autoclave from the oven, the product was slurried in 35 mL of DDI H₂O in a 50 mL centrifuge tube, and the solution was centrifuged and decanted. The resulting solids were slurried with 35 mL of acetone (Fisher), and centrifuged several times, until the supernatant was clear. The solids were then air-dried at 100 °C overnight.

4.4 Photocleavage of P-SDA 2 in As-Made Aluminophosphate and Metal-Substituted Aluminophosphate Materials

The as-made, crystalline, aluminophosphate and metal-substituted aluminophosphate materials were suspended in DDI H₂O via sonication for 5 min. and drop-coated onto glass slides bounded by sticky tape, and allowed to air-dry for 24 h. Using a UVP Blak-

Ray long-wave mercury arc lamp, the samples were irradiated for 6 h. After cleavage, the samples were scraped off the glass slides, and stirred for 2 h each with acetone (Fisher), chloroform (EMD), and ethyl acetate (EMD), filtering between each step, to extract the organic fragments.

4.5 Characterization

The materials were characterized using a combination of liquid-state ^1H and solid-state ^{13}C nuclear magnetic resonance (NMR), infrared spectroscopy (IR), thermogravimetric analysis (TGA), and powder X-ray diffraction (XRD). NMR analysis was carried out with a Varian Mercury 300 MHz spectrometer (liquid state) and a Bruker AM 300 MHz spectrometer (solid-state). IR analysis was carried out on a Nicolet Nexus 470 FTIR spectrometer. TGA was performed on a NETZSH STA 449C analyzer in air using an aluminum sample pan. XRD was carried out on a Scintag XDS 2000 diffractometer operated at -45 kV and 40mA using Cu K_α radiation ($\lambda = 1.54056 \text{ \AA}$) in the 2θ range of 2-40 at a step size of $0.5^\circ / \text{min}$. Porosity measurements were carried out on using nitrogen adsorption techniques with a Micromeritics ASAP 2000.

5. References

- ¹ Lee, H., Zones, S. I. & Davis, M. E. A combustion-free methodology for synthesizing zeolites and zeolite-like materials. *Nature* **425**, 385-388 (2003).
- ² Lee, H., Zones, S. I. & Davis, M. E. in *Recent Advances In The Science And Technology Of Zeolites And Related Materials, Pts A - C Vol. 154 Studies In Surface Science And Catalysis*, 102-109 (2004).
- ³ Lee, H., Zones, S. I. & Davis, M. E. Zeolite synthesis using degradable structure-directing agents and pore-filling agents. *J. Phys. Chem. B* **109**, 2187-2191 (2005).
- ⁴ Lee, H., Zones, S. I. & Davis, M. E. Synthesis of molecular sieves using ketal structure-directing agents and their degradation inside the pore space. *Microporous Mesoporous Mat.* **88**, 266-274 (2006).
- ⁵ Clark, T. *et al.* A new application of UV-ozone treatment in the preparation of substrate-supported, mesoporous thin films. *Chem. Mater.* **12**, 3879-3884 (2000).
- ⁶ Li, Q. H., Amweg, M. L., Yee, C. K., Navrotsky, A. & Parikh, A. N. Photochemical template removal and spatial patterning of zeolite MFI thin films using UV/ozone treatment. *Microporous Mesoporous Mat.* **87**, 45-51 (2005).
- ⁷ Cooper, E. R. *et al.* Ionic liquids and eutectic mixtures as solvent and template in synthesis of zeolite analogues. *Nature* **430**, 1012-1016, doi:10.1038/nature02860 (2004).
- ⁸ Yang, X. B., Cambor, M. A., Lee, Y., Liu, H. M. & Olson, D. H. Synthesis and crystal structure of As-synthesized and calcined pure silica zeolite ITQ-12. *J. Am. Chem. Soc.* **126**, 10403-10409 (2004).

- ⁹ Zones, S. I. & Burton, A. W. Diquaternary structure-directing agents built upon charged imidazolium ring centers and their use in synthesis of one-dimensional pore zeolites. *J. Mater. Chem.* **15**, 4215-4223, doi:10.1039/b500927h (2005).
- ¹⁰ Il'ichev, Y. V., Schworer, M. A. & Wirz, J. Photochemical reaction mechanisms of 2-nitrobenzyl compounds: Methyl ethers and caged ATP. *J. Am. Chem. Soc.* **126**, 4581-4595, doi:10.1021/ja039071z (2004).
- ¹¹ Piggott, A. M. & Karuso, P. Synthesis of a new hydrophilic o-nitrobenzyl photocleavable linker suitable for use in chemical proteomics. *Tetrahedron Lett.* **46**, 8241-8244, doi:10.1016/j.tetlet.2005.09.077 (2005).
- ¹² Pillai, V. N. R. Photoremovable Protecting Groups in Organic Synthesis. *Synthesis* **1980**, 1-27 (1980).
- ¹³ Cuberes, M. R., Morenomanas, M. & Trius, A. Alpha-Lithiation of N-arylmethylimidazoles and Triazoles - A General Method for the Synthesis of 1,2-diaryl-1-(N-azolyl)-ethanes. *Synthesis-Stuttgart*, 302-304 (1985).
- ¹⁴ Utzinger, G. E. N-substituierte Arylhydroxylamine und deren Umwandlungsprodukte. *Justus Liebigs Annalen der Chemie* **556**, 50-64 (1944).
- ¹⁵ Szostak, R. *Molecular Sieves: Principles of Synthesis and Identification*. 2nd ed., (Blackie Academic & Professional, 1998).
- ¹⁶ Greene, T. W. *Protective Groups in Organic Synthesis*. (John Wiley & Sons, Inc., 1981).
- ¹⁷ Morris, R. E., Burton, A. W., Bull, L. M. & Zones, S. I. SSZ-51 - A New Aluminophosphate Zeotype: Synthesis, Crystal Structure, NMR and Dehydration Properties. *Chem. Mater.* **16**, 2844-2851 (2004).

- ¹⁸ Baerlocher, C., Meier, W. M. & Olson, D. H. *Vol. 2006*. (International Zeolite Association, 2006).
- ¹⁹ Chen, J. S. *et al.* Cobalt-substituted Aluminophosphate Molecular-Sieves - X-Ray Absorption, Infrared Spectroscopic, and Catalytic Studies. *Chem. Mater.* **4**, 1373-1379 (1992).